

Estimating horizontal movement performance of patient beds and the impact on emergency evacuation time

Jaeyoung Kwak^{a,*}, Michael H. Lees^b, Wentong Cai^c, Ahmad Reza Pourghaderi^{d,f,a} and Marcus E.H. Ong^{e,f}

^aComplexity Institute, Nanyang Technological University, 61 Nanyang Drive, Singapore 637335, Singapore

^bInformatics Institute, University of Amsterdam, Science Park 904, Amsterdam 1098XH, The Netherlands

^cSchool of Computer Science and Engineering, Nanyang Technological University, 50 Nanyang Avenue, Singapore 639798, Singapore

^dHealth Systems Research Center (HSRC), Singapore Health Services, 31 Third Hospital Avenue, Singapore 168753, Singapore

^eDepartment of Emergency Medicine, Singapore General Hospital, Outram Road, Singapore 169608, Singapore

^fHealth Services and Systems Research (HSSR), Duke-NUS Medical School, 8 College Road, Singapore 169857, Singapore

ARTICLE INFO

Keywords:

Emergency evacuation
Patient bed
Turning movement
Fatigue effect
Movement duration

ABSTRACT

Emergency evacuation of patients from a hospital can be challenging in the event of a fire. Most emergency evacuation studies are based on the assumption that pedestrians are ambulant and can egress by themselves. However, this is often not the case during emergency evacuations in healthcare facilities such as hospitals and nursing homes. To investigate emergency evacuations in such healthcare facilities, we performed a series of controlled experiments to study the dynamics of patient beds in horizontal movement. We considered a patient bed because it is one of the commonly used devices to transport patients within healthcare facilities. Through a series of controlled experiments, we examined the change of velocity in corner turning movements and speed reductions in multiple trips between both ends of a straight corridor. Based on the experimental results, we then developed a mathematical model of total evacuation time prediction for a patient bed horizontally moving in a healthcare facility. Factoring uncertainty in the horizontal movement, we produced the probability distribution of movement duration and estimated the probability that an evacuation can be safely performed within certain amount of time. In addition, we predicted that the evacuation time would be longer than the prediction results from an existing model which assumes constant movement speed. Our results from the model demonstrated good agreement with our experimental results.

1. Introduction

Pedestrian emergency evacuation has been one of the central topics in the field of fire safety engineering. In case of life threatening incidents such as fire and hazardous chemical spills, a well-prepared emergency evacuation plan can efficiently move occupants to the assembly points with minimum amount of time and ensure the safety of evacuees. Based on the degree of required aid during egress, occupants can be categorized into ambulant and non-ambulant occupants. Ambulant occupants can egress to the place of safety without help from other occupants. On the other hand, non-ambulant occupants need help when they move, especially in case of an emergency. The non-ambulant occupants can be further categorized into subcategories such as bedridden occupants and wheelchair users depending on the device that they are using.

Emergency evacuation of ambulant pedestrians has been investigated in experimental studies to understand pedestrian movement during emergency evacuations. Numerous experiments have been conducted in horizontal evacuation scenarios in which pedestrians egress within the same floor. For instance, researchers have studied evacuations through bottlenecks to understand the relationship between the bottleneck width and pedestrian flow, which is critical to the total evacuation time in room evacuations [1, 2, 3]. A considerable

number of experiments have been performed to characterize pedestrian vertical movement through stairs such as downward moving speed and flow rate in a stairwell of a high-rise building [4] and the influence of stair slope on such pedestrian flow characteristics [5]. The pedestrian flow characteristics have been studied for harsh moving conditions including crawling in a room [6] and in a corridor [7], and the existence of earthquake-induced falling debris [8].

In most existing emergency evacuation studies, it is assumed that pedestrians are able to walk and egress by themselves. However, this is often not the case during emergency evacuations especially in healthcare facilities such as hospitals and nursing homes. Healthcare facilities accommodate considerable numbers of non-ambulant patients who have limited mobility and need the help of medical staff with evacuation devices during the evacuation process. To prepare emergency evacuation plans considering the non-ambulant pedestrians, it is necessary to understand the performance of evacuation devices such as their movement speed and movement dynamics.

Previous experimental studies of non-ambulant pedestrian evacuations analyzed video footage of the experiments to measure travel time between different reference points. By doing that, average movement speed was measured for different sections of an evacuation route such as a straight corridor and a stairwell. For example, Rubadiri *et al.* [9] performed a horizontal evacuation exercise of manual and electric wheelchair users. They measured the evacuation per-

*Corresponding author: Jaeyoung Kwak (jaeyoung.kwak@ntu.edu.sg)
ORCID(s):

formance index as a ratio of the wheelchair user movement speed without assistance to the movement speed of ambulant pedestrians. Based on the measured evacuation performance index, they predicted evacuation time of the wheelchair users and then compared it with the actual measurement of the wheelchair users. Strating [10] collected movement speed data of bedridden occupants in Dutch healthcare facilities. He reported an evacuation speed range from 0.54 to 1.34 m/s in Dutch hospitals and from 0.25 to 1.30 m/s in Dutch nursing homes. Hunt *et al.* [11] measured horizontal and vertical movement speed of evacuation devices including stretchers, evacuation chairs, carry chairs, and rescue sheets. They observed that the evacuation chair is the fastest among the tested evacuation devices with an average speed of 1.5 m/s in the horizontal evacuation and of 0.83 m/s in the vertical evacuation. Based on the measured movement speed of those evacuation devices, they also estimated the total evacuation time of non-ambulant patients in a high-rise hospital building. While those studies focused on measuring the average movement speed of non-ambulant pedestrian evacuation devices, change of velocity during the movement has not yet been studied in detail.

In pedestrian flow dynamics, it has been reported that pedestrians continuously moving with heavy load tend to have reduced movement speed due to fatigue [12]. Furthermore, several studies investigated speed profiles of pedestrians moving near obstacles in front of an exit [13], corners [14], and merging areas [15]. Such structural elements of pedestrian facilities often act as a constraint on the efficiency of pedestrian flow seemingly because pedestrians need to change their moving direction and speed.

Similar to the case of pedestrian flow dynamics, the movement of an evacuation device becomes slower when the device is moving in corners and areas of merging flow and interaction with other devices coming from different directions. In addition, there are often far more bedridden patients than medical staff in healthcare facilities. It is apparent that, in emergency evacuations, every medical staff needs to make multiple trips between the location of bedridden patients and the place of safety. One can expect that the medical staff experience some level of exhaustion when they evacuate all the bedridden patients and it is likely that their movement becomes slower as they travel longer distance. Such a slow-moving evacuation device affects the flow of subsequent evacuation devices and pedestrians, especially with limited passing opportunities in a narrow corridor. Consequently, understanding these non-linear dynamics of evacuation devices enables us to better estimate the evacuation performance of the devices with taking into account their speed profile and change of moving directions.

Among various evacuation devices, we considered the movement of a patient bed because it is one of the most commonly used devices to transport patients from one place to the another in healthcare facilities. In this study, we performed a series of controlled experiments to investigate the dynamics of patient beds in horizontal movement. Through the controlled experiments, we examined the change of ve-

locity in corner turning movements and speed reductions in multiple trips between both ends of a straight corridor. Based on the experimental results, we then developed a movement duration prediction model and then applied the model for a patient bed horizontally moving in a healthcare facility. Incorporating uncertainty in the horizontal movement, we predicted probability that an evacuation can be safely performed within certain amount of time. The experiment setup and data collection methods are described in Section 2. As shown in Section 3, we analyze the dynamics of patient bed movement, develop a movement duration prediction model, and then apply the model for a patient bed horizontally moving in a healthcare facility. We summarize the results with concluding remarks in Section 4.

2. Experiment setup

To collect patient bed movement data, we carried out a series of controlled experiments in September 2019 at the Singapore General Hospital, Singapore. In total, 4 males and 4 females aged between 25 to 35 without movement impairments took part in the experiments. In order to move a patient bed, the handlers were grouped into pairs of same gender handlers: male-male and female-female handlers. Additionally, one male (27 years old, 189 cm, 87 kg) was lying on the patient bed during its movement in order to substitute for a real non-ambulant patient. Before starting the experiment, the handlers had an orientation session and conducted a few warm-up trials to make them proficient enough in maneuvering the patient bed. In the experiment, we asked all the participants to move the patient bed as fast as possible while making sure their safety.

Figure 1 shows the sketches of the experiment setup: a 90° angled corner and a straight corridor. In the 90° angled corner setup, each handler pair was maneuvering a patient bed in the intersection of 2 m × 2 m and two straight corridors of 2 m wide 5 m long. Handlers made left-turning movements by moving from the top to the right branches, and from the right to the top branches for right-turning movements. The handler pair repeated right and left turning movement at least 10 times. In the straight corridor experiment setup, each handler pair made 21 round trips with a patient bed in a straight corridor of 2 m wide 21 m long. By doing that, the handler pair moved the patient bed a distance of 882 m in effect. In both experiment setups, there were not obstacles or doors on the experimental route. According to the usual practice [16], a pair of handlers was moving the patient bed together in both experiments. In each pair, one handler was acting as a leading handler who was guiding the movement direction of the bed, while the other handler was pushing the bed following the leading handler. Once the handlers reached the end of the experiment area, they changed their position in order to reverse their movement direction. The formation of handlers in each experiment setup is illustrated in Fig. 2.

Both experiments were recorded using cameras with a frame rate of 30 frames per second. The cameras were mounted

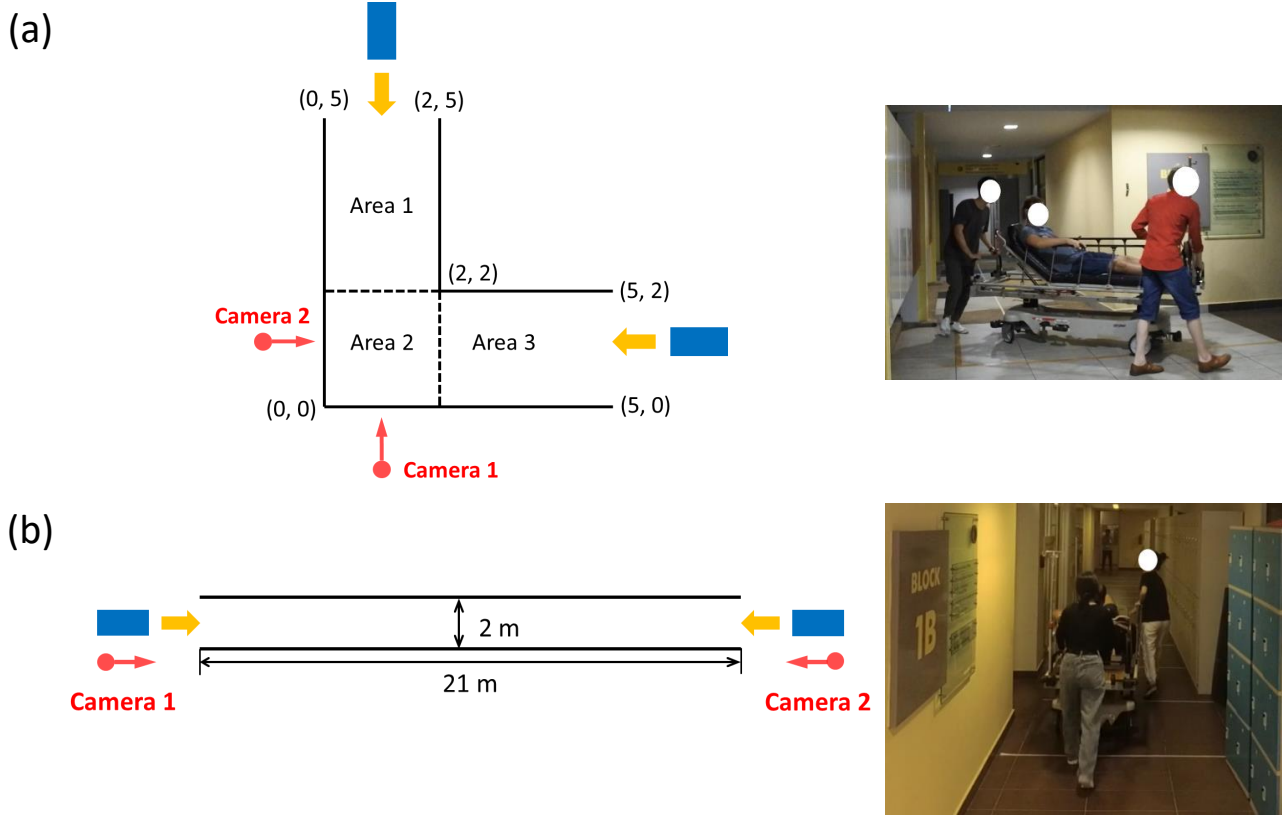


Figure 1: Schematic representation of experiment setup: (a) a 90° angled corner and (b) a straight corridor. In (a), Areas 1 and 3 indicate 3 m long 2 m wide straight corridor sections and Area 2 shows 2 m-by-2 m intersection. Blue rectangles depict patient beds and yellow arrows show their moving direction. Red circles and red arrows indicate the locations of cameras and their pointing direction, respectively.

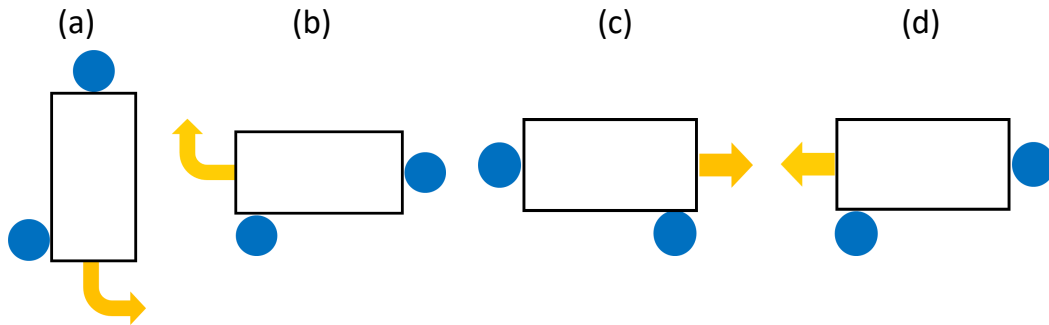


Figure 2: Schematic representation of handler positions with the direction of travel: (a) left-turning movement from the top to the right branches in the 90° angled corner setup, (b) right-turning movement from the right to the top branches in the 90° angled corner setup, (c) rightward movement in the straight corridor setup, and (d) leftward movement in the straight corridor setup. Blue circles depict handlers and yellow arrows show their moving direction.

on tripods which were set on the top of tables. In the 90° angled corner setup, we set two cameras near the corner to closely observe the turning movement of the patient bed. In the straight corridor setup, two cameras were used to record the bed movement from each end of the corridor. From video footage of the 90° angled corner setup, we extracted patient bed movement trajectories using T-analyst, a semi-automatic trajectory extraction software developed from Lund University, Sweden [17]. The software has been applied in cyclist traffic safety analysis [18] and pedestrian flow analysis [19]. The conversion from video coordinates to the real world co-

ordinates was performed by T-calibration, a calibration software accompanied by T-analyst. In T-calibration software, we placed calibration points and its real-world coordinates and then performed TSAI-calibration algorithm [20]. After the calibration process, we manually annotated pedestrian positions for every 10 frames on average in the video footage with T-analyst software. Next, T-analyst software then extracted pedestrian trajectories. Details of pedestrian trajectory extraction process can be found from T-analyst manual available from its webpage [17].

Table 1 shows the basic movement characteristics of han-

Table 1Basic movement characteristics of handler groups in the corner area of $x \leq 5$ and $y \leq 5$.

Handler groups	Gender	Movement direction	Orientation (rad)		No. of trajectories	Distance (m)	Duration (s)	Average speed (m/s)	Entering speed (m/s)
			starting	target					
LT_1	Female	Left turn	1.57	0	12	7.59 ± 0.16	10.59 ± 0.57	0.72 ± 0.03	0.80 ± 0.06
LT_2	Female	Left turn	1.57	0	13	7.45 ± 0.11	9.05 ± 0.67	0.83 ± 0.06	0.87 ± 0.09
LT_3	Male	Left turn	1.57	0	10	7.58 ± 0.12	10.17 ± 0.73	0.75 ± 0.05	0.72 ± 0.15
LT_4	Male	Left turn	1.57	0	15	7.59 ± 0.10	7.34 ± 1.04	1.05 ± 0.11	0.95 ± 0.12
RT_1	Female	Right turn	3.14	1.57	12	7.67 ± 0.06	9.13 ± 0.54	0.84 ± 0.05	1.15 ± 0.07
RT_2	Female	Right turn	3.14	1.57	13	7.59 ± 0.10	7.24 ± 0.42	1.05 ± 0.06	1.32 ± 0.11
RT_3	Male	Right turn	3.14	1.57	10	7.98 ± 0.12	9.33 ± 0.61	0.86 ± 0.04	1.05 ± 0.08
RT_4	Male	Right turn	3.14	1.57	15	7.82 ± 0.13	6.47 ± 0.56	1.22 ± 0.08	1.51 ± 0.24
Average						7.65 ± 0.19	8.51 ± 1.57	0.93 ± 0.18	1.07 ± 0.29

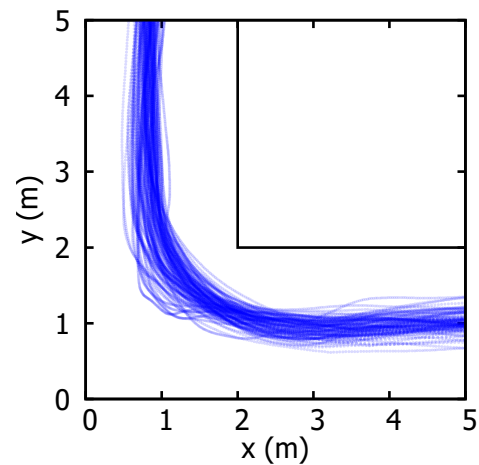
Table 2

Basic movement characteristics of handler groups in straight corridor experiment.

Handler groups	Gender	speed (m/s)		
		min.	max.	average
Group_1	Female	0.94	1.20	1.03
Group_2	Female	1.34	1.64	1.47
Group_3	Male	0.98	1.13	1.04
Group_4	Male	1.31	1.70	1.53

handler groups in the turning movement experiment. We collected 10 to 15 trajectories from each handler group and in total $N = 100$ trajectories were collected. The distance traveled and the movement duration were measured for each trajectory in the area of $x \leq 5$ and $y \leq 5$ and then averaged for each handler group. The average speed was computed by dividing the distance traveled by the movement duration. The entering speed was measured when the patient bed is entering the area of $x \leq 5$ and $y \leq 5$. Handler groups RT_2 and RT_4 showed shorter movement duration than other handler groups seemingly because they entered the corner with higher entering speed and experienced smaller speed drop in the course of their movement.

In the straight corridor setup, based on the study of Luo *et al.* [12], we assumed that the fatigue experienced by the handlers is affected by the distance that they transported the patient bed. The handlers were making multiple trips between one end to the other end of the corridor. We measured the time that the handlers took moving between the two ends of the corridor using the video footage. In doing that, we manually marked the transition period in which the handlers stopped and changed their position. After identifying the transition period, we obtained the travel time in each one-way trip and then calculated the average speed for each trip. The initial speed was measured from the first one-way trip in which the handlers moved first 21 meters in the straight corridor setup. Our approach of measuring the speed is analogous to the method presented by Chen *et al.* [21]. The average speed was measured by dividing the distance traveled (882 m) by the total travel time that the handlers moving the patient bed. Table 2 summarizes the basic movement characteristics of handler group in the straight corridor experiment.

**Figure 3:** $N = 100$ individual trajectories collected from the corner turning experiment setup

Handler groups Group_2 and Group_4 showed higher speed but there is not significant difference between male and female. The differences between the groups in the same gender (Group_1 vs. Group_2, and Group_3 vs. Group_4 in Table 2) seemingly attribute to the degree of risk aversion set by different groups. Although we asked all the participants to move as fast as possible, some of them might want to more focus on moving safely without getting injured, so they were not necessarily in a rush.

3. Results and analysis

3.1. Turning movement

Figure 3 shows individual trajectories collected from the corner turning experiment setup. To understand the change of velocity in the course of turning movement, we firstly obtained the average path of all the handler groups moving in both movement directions. Similar to Hicheur *et al.* [22], we resampled the collected trajectories into $N_f = 60$ equal intervals and then averaged the resampled trajectories for each

rescaled time point $\hat{t} \in [0, 1]$:

$$\begin{aligned} x_{avg}(\hat{t}) &= \frac{1}{N} \sum_{i=1}^N x_i(\hat{t}), \\ y_{avg}(\hat{t}) &= \frac{1}{N} \sum_{i=1}^N y_i(\hat{t}). \end{aligned} \quad (1)$$

Here, $N = 100$ is the number of collected trajectories from handler groups shown in Table 1. Likewise, we calculated trajectory deviation $\sigma(\hat{t})$ to quantify the difference between the mean trajectory and an individual trajectory i :

$$\sigma_x(\hat{t}) = \sqrt{\frac{1}{N} \sum_{i=1}^N (x_i(\hat{t}) - x_{avg}(\hat{t}))^2}, \quad (2)$$

$$\sigma_y(\hat{t}) = \sqrt{\frac{1}{N} \sum_{i=1}^N (y_i(\hat{t}) - y_{avg}(\hat{t}))^2}, \quad (3)$$

$$\sigma(\hat{t}) = \sqrt{\sigma_x^2(\hat{t}) + \sigma_y^2(\hat{t})}. \quad (4)$$

By making use of the rescaled time points, we identified start and end of turning movement. We measured the angular displacement θ and its average θ_{avg} :

$$\begin{aligned} \theta(\hat{t}_j) &= \arccos\left(\frac{\vec{e}_0 \vec{e}_i}{\|\vec{e}_0\| \|\vec{e}_i\|}\right), \\ \theta_{avg}(\hat{t}_j) &= \frac{1}{N} \sum_{j=1}^N \theta(\hat{t}_j), \end{aligned} \quad (5)$$

where \vec{e}_0 is the initial moving direction which is set as (0, -1) for left-turn movement and (-1, 0) for right-turn movement. The moving direction at rescaled time \hat{t}_j is given as $\vec{e}_i = (\Delta x / \Delta l, \Delta y / \Delta l)$. Here, Δx and Δy denote the difference between the values of x_i and y_i at the current rescaled time points \hat{t}_j and the previous rescaled time point \hat{t}_{j-1} . The displacement between the positions at rescaled time \hat{t}_j and \hat{t}_{j-1} is given as $\Delta l = \sqrt{\Delta x^2 + \Delta y^2}$.

Figure 4(a) presents angular displacement of the patient bed against rescaled time points. One can observe that the angular displacement curve is nearly straight between $\hat{t} = 0.358$ and $\hat{t} = 0.658$, indicating that the patient bed is turning with a constant angular speed $0.24 \text{ rad}/\hat{t}$. When the patient bed starts and ends the turning movement, either $\sigma_x(\hat{t})$ or $\sigma_y(\hat{t})$ is at peak value. Figures 4(b) and 4(c) indicate that the start and end of turning movement can be identified based on the components of trajectory deviation, i.e., $\sigma_x(\hat{t})$ and $\sigma_y(\hat{t})$.

The identified locations of turning movement start and end are presented with the mean trajectory in Fig. 5. Similar to work of Dias *et al.* [23], it was observed that the turning movement started before and ended after Area 2 ($x \leq 2$ and $y \leq 2$).

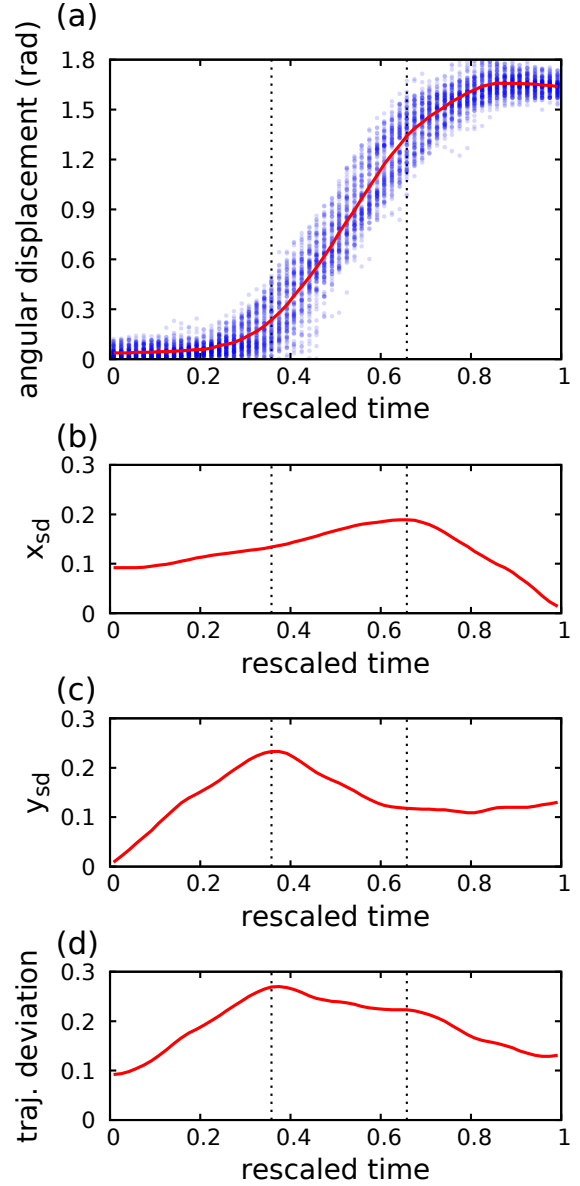


Figure 4: Angular displacement of the patient bed: (a) individual angular displacement (blue circles) and the average value (red solid line). Black dashed lines indicate start (left dashed line) and end (right dashed line) of turning movement. (b)-(d) the corresponding graphs of $\sigma_x(\hat{t})$, $\sigma_y(\hat{t})$, and $\sigma(\hat{t})$. It can be observed that the start and end of turning movement occur when either $\sigma_x(\hat{t})$ or $\sigma_y(\hat{t})$ is at peak value.

Figure 6(a) shows examples of individual speed curves before resampling. Due to various initial speed and maneuvering duration, it is difficult to understand patterns in the speed curves. We applied the idea of the rescaled time points to such speed curves. We resampled the instantaneous speed v_i of individual handler groups into N_f equal intervals and then averaged the resampled speed for each rescaled time point $\hat{t} \in [0, 1]$:

$$v_{avg}(\hat{t}) = \frac{1}{N} \sum_{i=1}^N v_i(\hat{t}). \quad (6)$$

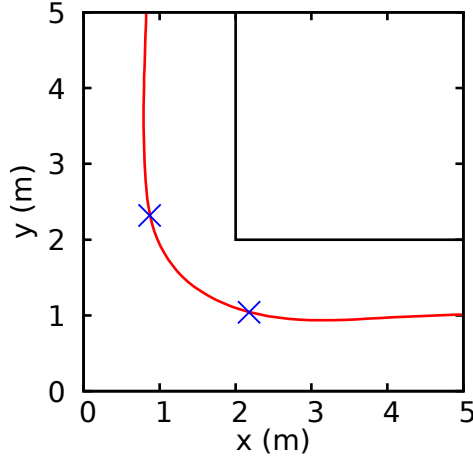


Figure 5: Average path (red solid line) with the locations of turning movement start and end (blue cross symbols).

In order to compare different speed curves, we normalized the speed curves with entering speed v_0 . Figure 6(b) presents the result of normalization performed against rescaled time \hat{t} for curves in Fig. 6(a). We performed normalization for $N = 100$ individual speed curves and then averaged their normalized speed in rescaled time space. Figure 6(c) illustrates the average of normalized speed curves and its trend line. The trend line is generated by the normalized speed profile $\hat{v}(\hat{t})$.

According to minimum jerk principle (Hogan [24] and Pham *et al.* [25]), people tend to minimize jerk (i.e., a third-order derivative of position) while turning around a corner:

$$\int_0^1 \left[\left(\frac{d^3 x}{d\hat{t}^3} \right)^2 + \left(\frac{d^3 y}{d\hat{t}^3} \right)^2 \right] d\hat{t}, \quad (7)$$

where x and y represent position in x - and y -axis at a rescaled time point \hat{t} . Based on the minimum jerk principle, the normalized speed profile $\hat{v}(\hat{t})$ can be represented by a fourth-order polynomial equation of rescaled time point \hat{t} :

$$\hat{v}(\hat{t}) = a_0 + a_1 \hat{t} + a_2 \hat{t}^2 + a_3 \hat{t}^3 + a_4 \hat{t}^4. \quad (8)$$

The coefficients a_0 , a_1 , a_2 , a_3 , and a_4 can be determined from the average of normalized speed curves in Fig. 6(c). Table 3 shows the coefficient values. Following the work of Dias *et al.* [26], we modeled the normalized speed profile $\hat{v}(\hat{t})$ with the same values in the start and end of the curve: $\hat{v}(0) = 1$ and $\hat{v}(1) = 1$.

3.2. Fatigue effect

As stated in the last paragraph of Section 2, we measured the travel time in each one-way trip and then calculated the average speed for each trip. The handler group speed in the straight corridor setup is shown in Fig. 7. As can be seen from Fig. 7, one can observe that the handler group movement speed decreases as the distance traveled s increases, especially for first 300 m.

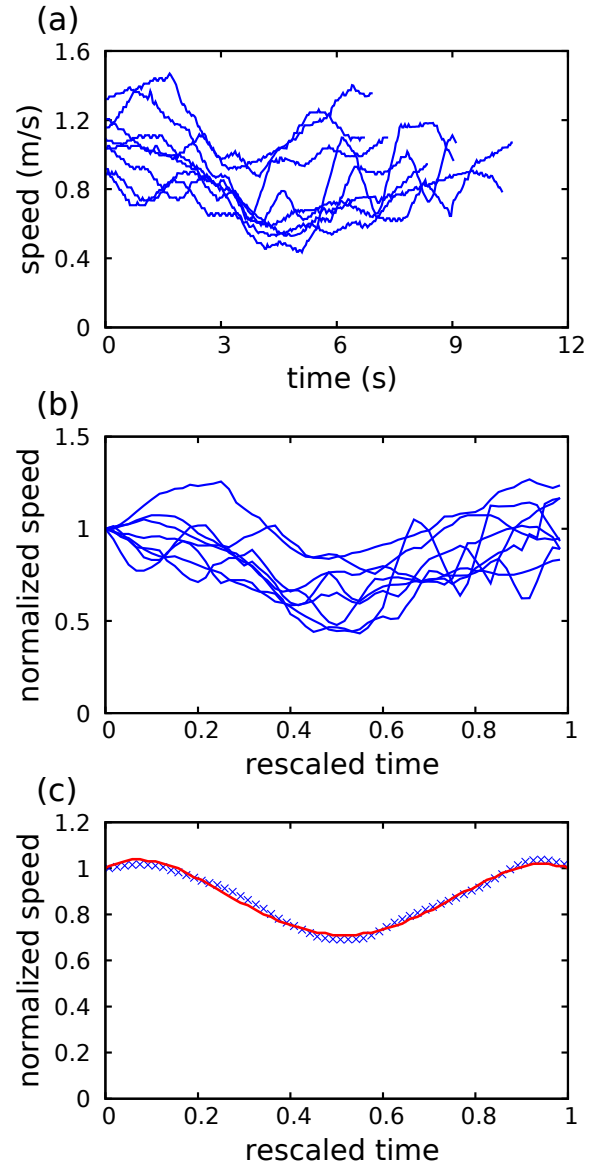


Figure 6: Speed profile of handler groups as a function of rescaled time in the area of $x \leq 5$ and $y \leq 5$: (a) examples of individual speed curves. (b) the result of normalization performed against rescaled time \hat{t} for curves in (a). (c) the average of normalized speed curves (blue cross symbols) with its trend line (red solid line). The trend line begins to decrease and then increase when the patient bed is turning around a corner.

To further quantify the tendency of decreasing travel speed due to fatigue effect, we evaluated the fatigue coefficient f_a based on the speed reduction with respect to the initial movement speed v_0 . According to the work of Luo *et al.* [12], the fatigue coefficient f_a is given as:

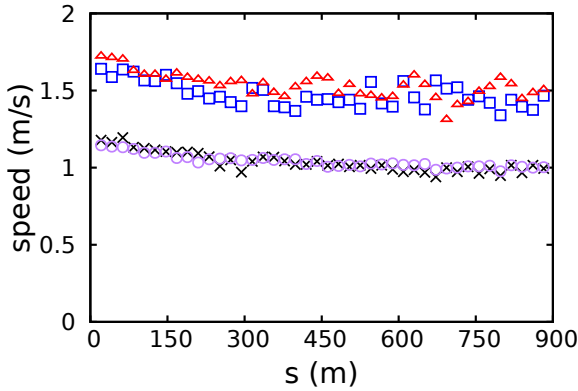
$$f_a = \frac{v_0 - v_i}{v_0}. \quad (9)$$

Here, v_i indicates the current speed which was calculated for each one-way trip from one end to the other end of the straight corridor (see Fig. 1(b)). As shown in Eq. (9), the fatigue coefficient examines speed reduction ratio, so the fa-

Table 3

Normalized speed profile coefficients

Coefficient	Value
a_0	1
a_1	1.1651
a_2	-10.0789
a_3	17.4769
a_4	-8.5632

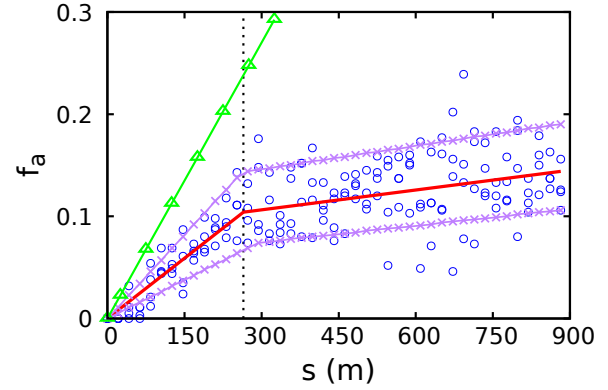
**Figure 7:** The handler group movement speed in the straight corridor setup. Different symbols represent the speed of different handler groups: black cross (×) for Group_1, blue rectangle (□) for Group_2, purple circle (○) for Group_3, and red triangle (△) for Group_4.

tigue effect can be compared among different handler groups even if they have different speed. In addition, the concept of fatigue coefficient is useful when one wants to estimate the speed at a certain traversed distance based on the initial speed. Based on Eq. (9), we evaluated the fatigue coefficient f_a for each handler group indicated in Table 2. Note that the current speed v_i and fatigue coefficient f_a are given as functions of distance traveled s , and v_i is the average speed calculated from each one-way trip. Figure 8 shows the relationship between f_a and s . One can observe that the fatigue coefficient values tend to rapidly increase in the beginning and then slowly grow. That is compatible with the decreasing trend of handler group movement speed shown in Fig. 7.

We applied piecewise linear regression [27] to quantify those two regimes in the fatigue coefficient curve:

$$f_a(s) = \begin{cases} \beta_1 s & \text{if } s \leq s_x \\ \beta_1 s + \beta_2 (s - s_x) & \text{if } s > s_x \end{cases} \quad (10)$$

where s_x is the breakpoint and β_1 and β_2 are regression coefficients. We used *nls* function in R package to fit the piecewise linear regression model in Eq. (10). It was estimated that the fatigue coefficient f_a curve slope changes at breakpoint $s_x = 264.4$ m. The slope for the first and second segments are estimated as $\beta_1 = 4.076 \times 10^{-4}$ and $\beta_1 + \beta_2 = 5.84 \times 10^{-5}$, respectively. The slope coefficients β_1 and $\beta_1 + \beta_2$ indicate that, the speed decreases by roughly 4.08% and 0.58% on average for each increase of 100 m in

**Figure 8:** Relationship between the fatigue coefficient f_a and the distance traveled s . The measured fatigue coefficient f_a from handler groups is denoted by blue circles (○). The corresponding trend line is indicated by red solid line. Black dashed line indicates the breakpoint location $s_x = 264.4$ m at which fatigue coefficient f_a curve slope changes. Purple solid lines with cross symbols (×) show the boundaries of 80% prediction band with quantiles 0.10 and 0.90. The fatigue coefficient curve of Luo *et al.* [12] is denoted by green solid line with triangles (△). In their study, f_a was measured for pedestrians carrying heavy items (10~20 kg) by hand.**Table 4**

The fatigue coefficients estimated by piecewise linear regression: the breakpoint and slopes.

Coefficient	Value
s_x	264.4 ± 24.7
β_1	4.076×10^{-4}
β_2	-3.492×10^{-4}
$\beta_1 + \beta_2$	5.840×10^{-5}

Table 5

The slope coefficients estimated by piecewise linear quantile regression for 80% prediction band with quantiles 0.10 and 0.90.

Coefficient	Quantiles	
	0.1	0.9
β_1	2.520×10^{-4}	5.476×10^{-4}
β_2	-1.976×10^{-4}	-4.714×10^{-4}
$\beta_1 + \beta_2$	5.447×10^{-5}	7.619×10^{-5}

distance traveled for $s \leq s_x$ and $s > s_x$, respectively. Table 4 depicts the fatigue coefficients estimated by piecewise linear regression including the breakpoint and slopes. In addition, we also applied *quantreg* function in R package to perform piecewise linear quantile regression based on Eq. (10) in order to generate 80% prediction band showing possible upper and lower boundaries of data points. Table 5 depicts the slope coefficients estimated by piecewise linear quantile regression for 80% prediction band with quantiles 0.10 and 0.90.

We compared the value of fatigue coefficient f_a obtained

in this study with that one reported in the study of Luo *et al.* [12]. In their study, the handlers were walking on a circular track while carrying heavy items (10~20 kg) by hand. For the same initial speed (between 1.25 m/s and 1.75 m/s), at distance of 325 m, the value of f_a measured in this study ($f_a = 0.11$) is lower than the value ($f_a = 0.42$) reported by Luo *et al.* [12]. This is seemingly because maneuvering a patient bed is physically less demanding than carrying heavy items by hand while walking. Although the data points obtained from this study are scattered in Fig. 8, it still clearly illustrates the tendency of increasing fatigue coefficient f_a as the distance s increases.

3.3. Prediction of movement duration

Based on the average normalized speed curves shown in Fig. 6(c), we can predict the movement duration of a patient bed in the corner area (i.e., $x \leq 5$ and $y \leq 5$). We describe the distance traveled in the corner area s_c with the following equation:

$$\begin{aligned} s_c &= \sum_{i=1}^{N_t} v_i \Delta t_i \\ &= \Delta t_i \sum_{i=1}^{N_t} v_i, \end{aligned} \quad (11)$$

where N_t is the number of intervals and v_i is the speed at interval i . The interval length Δt_i can be obtained by rearranging Eq. (11):

$$\Delta t_i = \frac{s_c}{\sum_{i=1}^{N_t} v_i}. \quad (12)$$

The movement duration in the corner area t_c is a summation of Δt_i ,

$$\begin{aligned} t_c &= \sum_{i=1}^{N_t} \Delta t_i \\ &= N_t \Delta t_i. \end{aligned} \quad (13)$$

The speed at interval i can be obtained from \hat{v}_i by multiplying entering speed v_0 , i.e., $v_i = v_0 \hat{v}_i$. Here, \hat{v}_i is normalized speed profile \hat{v} at interval i . The movement duration in the corner area t_c is given as:

$$t_c = \frac{s_c N_t}{v_0 \sum_{i=1}^{N_t} \hat{v}_i}. \quad (14)$$

The average normalized speed profile \hat{v}_{avg} is given as:

$$\hat{v}_{avg} = \frac{1}{N_t} \sum_{i=1}^{N_t} \hat{v}_i \quad (15)$$

Table 6

Probabilistic model input parameters.

parameters	mean	sd	min	max
s_c	7.65	0.19	7.27	8.03
v_0	1.07	0.29	0.49	1.65

and if we approximate Eq. (15) to continuous space by utilizing Eq. (8), \hat{v}_{avg} becomes

$$\begin{aligned} \hat{v}_{avg} &= \int_0^1 \hat{v}_i d\hat{t} \\ &= a_0 \hat{t} + \frac{1}{2} a_1 \hat{t}^2 + \frac{1}{3} a_2 \hat{t}^3 + \frac{1}{4} a_3 \hat{t}^4 + \frac{1}{5} a_4 \hat{t}^5 \Big|_0^1 \quad (16) \\ &= \left(a_0 + \frac{1}{2} a_1 + \frac{1}{3} a_2 + \frac{1}{4} a_3 + \frac{1}{5} a_4 \right). \end{aligned}$$

Accordingly, Eq. (14) should read

$$t_c = \frac{s_c}{v_0 \hat{v}_{avg}}. \quad (17)$$

Here, distance traveled in the corner area s_c , entering speed v_0 , and average normalized speed profile \hat{v}_{avg} are input parameters. Based on Eq. (16), we can obtain $\hat{v}_{avg} = 0.874$.

In order to reflect uncertainty in the movement duration of a bedridden patient (see Eq. (17)), we developed a probabilistic model based on the input parameters s_c and v_0 for movement duration prediction. Previous studies [28, 29] noted that a probabilistic approach is beneficial to estimate evacuation time based on an empirical predictive model utilizing experimental data, especially when there exists notable variability in evacuation parameters such as premovement time and movement time. In the presented experimental results, one can notice that the difference in basic movement characteristics among handlers is considerable, thus our prediction model was developed in line with the probabilistic approach. Analogous to previous studies [9, 10, 11], the evacuation in this study refers to the movement of a bedridden patient moving with a group of handlers to the place of safety.

In the development of probabilistic prediction model, we assumed that s_c and v_0 follow Gaussian distribution. Table 6 shows the probabilistic model input parameters. We set the mean and standard deviation values of the input parameters same as in the experimental results. The maximum and minimum values were determined by adding and subtracting twice of the standard deviation to and from the mean value, respectively. Based on Eq. (17) with the probabilistic model input parameters in Table 6, we performed 1000 simulations. The frequency histogram of the movement duration is shown in Fig. 9, which has a mean of 8.85 s and a standard deviation of 2.79 s. Its range is [5.01, 18.62] s. The experimental results of movement duration [5.67, 11.80] s all fall within the simulated distribution. This indicates that our prediction model of movement duration can successfully replicate the experimental data of movement duration.

In order to reflect the effect of fatigue on travel time, we considered the fatigue coefficient f_a and the relationship

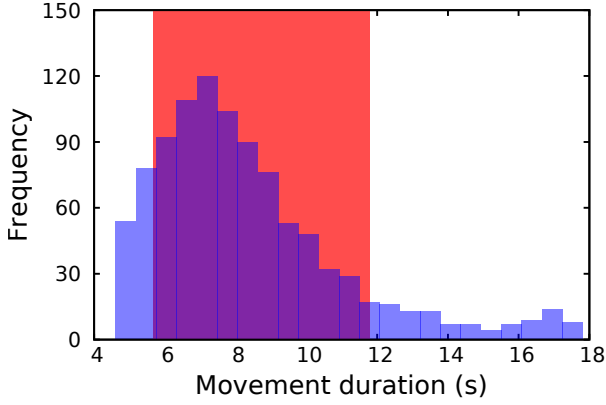


Figure 9: Frequency histogram of movement duration in a corner area estimated from numerical simulation. Red shaded area indicates the range of movement duration measured from the experiment.

with the distance traveled s in the estimation of movement duration. Like Eq. (13), the movement duration in a straight corridor t_s is given as

$$t_s = \sum_{i=1}^{N_s} \Delta t_j, \quad (18)$$

where Δt_j is the travel time in segment j and N_s is the number of segments. Note that Δt_j is not constant here, meaning that the travel speed is different for each segment. The normalized speed \hat{v} is obtained after we rearranged Eq. (9),

$$\hat{v} = \frac{v}{v_0} = 1 - f_a, \quad (19)$$

again, v_0 is entering speed. The average travel speed in segment j is given as

$$\frac{\Delta s_j}{\Delta t_j} = \frac{v_{j-1} + v_j}{2}, \quad (20)$$

where Δs_j is the distance traveled in segment j and v_{j-1} is the speed at the beginning point of segment j and v_j for the end point of segment j . After combining Eqs. (19) and (20), we obtained the travel time of segment j as

$$\Delta t_j = \frac{\Delta s_j}{v_0} \left(\frac{2}{\hat{v}_{j-1} + \hat{v}_j} \right). \quad (21)$$

3.4. Case study: Singapore General Hospital Emergency Department

In this case study, we demonstrate how the presented approach can be applied to predict the movement duration of a handler group transporting multiple bedridden patients. We selected the current Singapore General Hospital Emergency Department (SGH ED) for the case study. In Fig. 10, we present a schematic representation of the bedridden patient evacuation route in the current SGH ED. The evacuation route starts from the critical care unit (CCU) at (0,0)

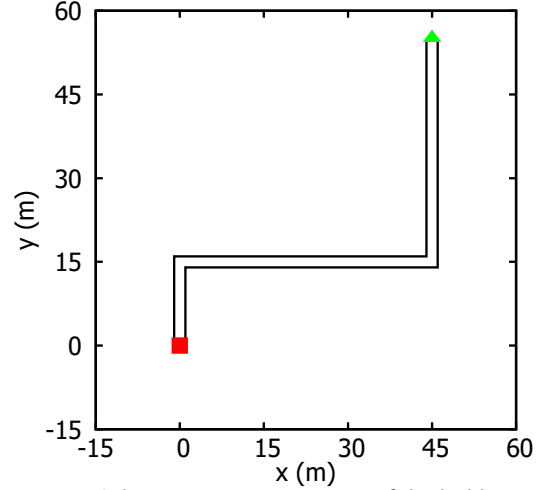


Figure 10: Schematic representation of bedridden patient evacuation route in current Singapore General Hospital Emergency Department (SGH ED). The evacuation route starts from the critical care unit (red square) which is placed at (0,0) to the place of safety (green triangle) at (45,55). The evacuation route includes three straight corridor sections and two corner areas. The evacuation route is 2 m wide, same as the experiment condition.

Table 7

Bedridden patient evacuation route segments

	Segment type	from	to	Length (m)
1	Straight corridor	(0, 0)	(0, 11)	11
2	Corner	(0, 11)	(4, 15)	7.65 ± 0.19
3	Straight corridor	(4, 15)	(41, 15)	37
4	Corner	(41, 15)	(45, 19)	7.65 ± 0.19
5	Straight corridor	(45, 19)	(45, 55)	36

to the place of safety at (45,55). The evacuation route is 2 m wide (the same width as our experiment condition), and includes three straight corridor sections and two corner areas, as shown in Table 7. Note that we modeled CCU and the place of safety as single points in order to focus on the evacuation of bedridden patients between those areas. The actual geometry of the areas is much more complicated, thus the movement duration within the areas is not considered for simplicity. As in Section 3.3, the evacuation time in this case study was estimated for a patient bed moving with two handlers. Another important point to note is that evacuation of a bedridden patient with a handler group cannot be simply extended to the case of a population of bedridden patients with multiple handler groups. This is mainly because the interactions among the handler groups are likely to affect their movement speed.

We estimated the movement duration of a handler group carrying a bedridden patient from CCU to the place of safety five times. It is reasonable to suppose that the handler group in this case study were expected to move the patient bed as fast as possible and their movement characteristics are the same as in the experimental study. Equations (17) and (21)

Table 8
Probabilistic model input parameters.

parameters	mean	sd	min	max
s_c	7.65	0.19	7.27	8.03
v_0	1.07	0.29	0.49	1.65
t_p	7.96	5.19	4.10	17.64
t_q	6.25	2.60	2.54	10.25
s_x	264.4	24.7	215.0	313.8
β_1	4.076×10^{-4}	7.780×10^{-5}	2.520×10^{-4}	5.476×10^{-4}
β_2	-3.492×10^{-4}	7.580×10^{-5}	-4.714×10^{-4}	-1.976×10^{-4}
$\beta_1 + \beta_2$	5.840×10^{-5}	8.895×10^{-6}	5.447×10^{-5}	7.619×10^{-5}

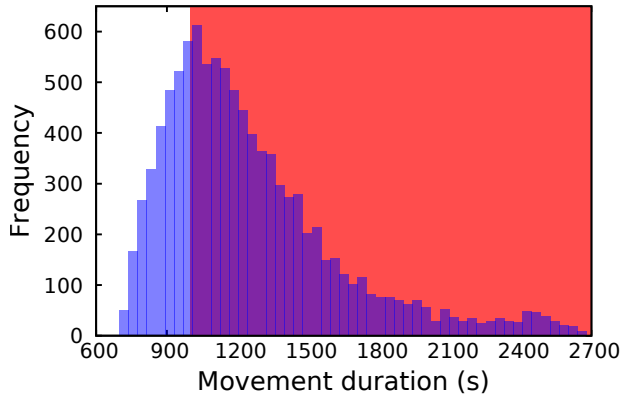


Figure 11: Numerical simulation results of movement duration for five round trips between CCU and the place of safety. The probability of finishing the movement within the reference time $T_{ref} = 999.09$ s is 23.6%. However, 76.4% of prediction results are longer than the reference time (indicated by the red shaded area), indicating that the reference time is not likely to be achievable. Here, the reference time T_{ref} is computed with the traditional deterministic evaluation method using the mean value of input parameters.

were applied to estimate the movement duration in the corner areas and straight corridor sections, respectively. We assumed that the fatigue effect is in effect both in the outgoing and return trips to the CCU, thus we applied the same fatigue coefficient function in Eq. (10) for the both trips.

In addition to the distance traveled in the corner area s_c and entering speed v_0 shown in Table 6, we introduced additional input parameters to the probabilistic model: preparation time t_p , positioning time t_q , breakpoint s_x , and fatigue coefficient curve slopes β_1 and β_2 . The preparation time is length of time required to prepare a patient bed for movement from CCU and the positioning time is the time taken to place a patient bed at the place of safety after its arrival. We set the mean and standard deviation of t_p and t_q based on the observation reported by Strating (2013) [10], and based on Tables 4 and 5 for s_x , β_1 , β_2 , and $\beta_1 + \beta_2$.

Based on our movement duration prediction model with the probabilistic model input parameters in Table 8, we performed 10000 simulations. In each simulation, the handler

Table 9

The probability and the corresponding available safe egress time (ASET) that a handler group can safely evacuate five bedridden patients. Note that the handler group can transport one bedridden patient to the place of safety for each round trip.

Probability	corresponding ASET (s)
10%	892.89
20%	973.72
30%	1041.17
40%	1109.65
50%	1181.31
60%	1266.27
70%	1368.30
80%	1506.48
90%	1773.08

group makes five round trips between CCU and the place of safety. The frequency of histogram of the movement duration is shown in Fig. 11, which has a mean of 1272.5 s and a standard deviation of 375.46 s. The estimated movement duration ranges from 718.1 s to 2699.7 s. One can observe a large spread of the numerical simulation results presented in Fig. 11 due to the right-skewed distributions of t_c and t_s . We refer the readers to Appendix A for further details.

By introducing a probabilistic model of movement duration prediction, we can consider the effect of uncertain factors in evacuation process, like entering speed, preparation time, positioning time, and fatigue effect coefficients. Based on the results shown in Fig. 11, one can estimate the probability that an evacuation can be safely performed within certain amount of time. Table 9 shows the probability and the corresponding available safe egress time (ASET) that a handler group can safely evacuate five bedridden patients. Note that the handler group can transport one bedridden patient to the place of safety for each round trip. For instance, the probability of successful evacuation is estimated as 90% if ASET is 1773.08 s. In fire evacuation studies, ASET is the

duration measured from the start of a fire to the onset of hazardous conditions in which people cannot be evacuated due to the fire. ASET is influenced by various factors including fire detection devices, location of fire origin, growth of fire, and ventilation paths [30].

In order to quantify the effect of uncertainty in the input parameters, we compared the movement duration prediction results against the reference time which is based on the traditional deterministic evaluation method. As stated in Zhang *et al.* [29], the value of reference time was computed based on the mean value of input parameters: evacuation route length ($l = 99.3$ m), preparation time ($t_p = 7.96$ s), positioning time ($t_q = 6.25$ s), and entering speed ($v_0 = 1.07$ m/s). For a handler group making five round trips between CCU and the place of safety, the reference time T_{ref} is computed as

$$T_{ref} = M(t_p + t_q + t_t), \quad (22)$$

where M is the number of round trips that the handler group makes and $t_t = 2l/v_0$ is the time required for the handler group to make a round trip between CCU and the place of safety excluding the time for preparation and positioning. As can be seen from Fig. 11, the probability that the handlers evacuate five bedridden patients within the reference time $T_{ref} = 999.09$ s is 23.6% while 76.4% of prediction results are longer than the reference time. It appears that the traditional deterministic evaluation method based on the mean value of input parameters underestimates the movement duration.

4. Conclusion

We performed a series of controlled experiments to study the dynamics of patient beds in horizontal movement. In our experiments, we examined the change of velocity in corner turning movements and speed reductions in multiple trips between both ends of a straight corridor. In the corner turning movements, we observed that the start and end of turning movement can be identified based on the trajectory deviation. We also quantified common patterns in different speed curves by means of the normalized speed profile with rescaled time. In the straight corridor experiment, we discovered experimental relationship between the fatigue coefficient and distance traveled $s \leq 882$ m. Based on the experiment results, we developed a movement duration prediction model and then applied the model for a patient bed horizontally moving in a healthcare facility. In order to reflect uncertainty in the horizontal movement, we introduced a probability distribution to the horizontal movement parameters like entering speed, preparation and positioning time, and fatigue coefficients. According to our case study results, one can estimate the probability that an evacuation can be safely performed within certain amount of time. In addition, it is highly probable that the horizontal movement duration would be longer than the prediction results from an existing model which assumes constant movement speed. The case study results demonstrated that our model has potential

in predicting emergency evacuation time of patient beds in healthcare facilities.

This study presents the experiment results from four handler groups in left and right turning movements, and the straight corridor movements, respectively. The experiment data was collected from a small number of handlers and they are all young adults who are not professionally trained. When we set up the experiment, we were mainly interested in observing difference in male and female groups, so we did not consider a group of mixed genders. In addition, the weight of the bedridden patient was fixed. The experiment results might be different for various age groups, the mix of genders in the handler groups, bedridden patient weight, and handlers' proficiency in moving patient beds. It is also noted that the handlers in the experiment were not necessarily in a rush as they would be in the real emergency evacuation. Thus, there exists the possibility that the movement speed of handlers in the real emergency evacuation can be higher than the speed reported in this study. The presented experiment results can be generalized with larger number of handler groups having different conditions like age and proficiency.

As a first step to study the dynamics of patient bed movement in horizontal space, we focused on the case of a patient bed movement based on simple experiment setups. Further experimental studies need to be carried out in order to extend the presented model. In emergency evacuations in healthcare facilities, there are several dozens of patient beds to be transported to the place of safety by multiple handler groups. During the evacuations, several patient beds are likely to move in the same evacuation route at the same time and the interactions among them might affect the movement speed. The examples of observable interactions include the distance between two moving patient beds and the acceleration and deceleration in their speed profile. Future studies can be also planned from the perspective of emergency evacuation simulations. Hunt *et al.* [31] pointed out that the movement of evacuation devices has not been appropriately considered in existing evacuation simulation models although the movement of such devices is critical for vulnerable patients. We are currently developing an evacuation simulation model that can incorporate our findings in patient bed movement dynamics to explicitly reflect their movement during the emergency evacuations in healthcare facilities. The evacuation simulation models can check potential conflict with other evacuees and geometric elements such as doors and corners, and predict the total evacuation time for the scenarios in which patient beds are fleeing with other evacuees. Another interesting extension of the presented study is to optimize the evacuation time of bedridden patients in healthcare facilities. The optimization study can be performed to design optimal evacuation routes and estimate the number of handlers for transporting patient beds to the place of safety.

Acknowledgements

This research is supported by National Research Foundation (NRF) Singapore, GOVTECH under its Virtual Singapore program Grant No. NRF2017VSG-AT3DCM001-031. The experiment was organized with the help of Ms. Yogeswary Pasupathi (Research nurse at the Singapore General Hospital Emergency Department) and members of Complexity Institute, Nanyang Technological University, Singapore. We thank Mr. Joshua for his help in processing video records.

A. Distribution of movement duration

In Sections 3.3 and 3.4, we presented the distribution of movement duration in a corner area and in the case study, respectively (see Figs. 9 and 11). This appendix provides evidence to suggest that the spread of movement duration can be large.

According to the setup of our numerical simulation study presented in Section 3.4, the movement duration T_1 for a round trip is given as a sum of preparation time t_p , positioning time t_q , and total travel time in the corner areas $t_c = \sum t_{c,i}$, and total travel time in the straight corridors $t_s = \sum t_{s,j}$:

$$\begin{aligned} T_1 &= t_p + t_q + t_c + t_s \\ &= t_p + t_q + \sum_{i=1}^{N_c} t_{c,i} + \sum_{j=1}^{N_s} t_{s,j}, \end{aligned} \quad (23)$$

where $N_c = 4$ is the number of corner areas in a round trip and N_s is the number of straight corridor segments in a round trip. Travel time in corner area i is denoted by $t_{c,i}$ and $t_{s,j}$ for straight corridor section j . Parameters t_p and t_q were assumed to follow normal distribution. The distribution of t_c can be explained by means of the ratio distribution and the distribution of t_s can be approximated by the reciprocal normal distribution.

As presented in Eq. (17), travel time in corner area i is given as

$$t_{c,i} = \frac{s_c}{v_0 \hat{v}_{avg}}. \quad (24)$$

Here, the distance traveled in the corner area s_c and the entering speed v_0 are assumed to follow the normal distribution while the average normalized speed profile \hat{v}_{avg} is set as a fixed value based on the experimental study result. That is, $t_{c,i}$ follows a distribution of a ratio of two independent normally distributed variables s_c and v_0 . According to Curtiss [32] and Springer [33], the ratio distribution of $t_{c,i}$ can be described by means of the joint distribution of s_c and v_0 :

$$\begin{aligned} f(s_c, v_0) &= \frac{1}{2\pi\sigma_{s,c}\sigma_{v,0}} \times \\ &\exp \left\{ -\frac{1}{2} \left[\left(\frac{s_c - \mu_{s,c}}{\sigma_{s,c}} \right)^2 + \left(\frac{v_0 - \mu_{v,0}}{\sigma_{v,0}} \right)^2 \right] \right\}, \end{aligned}$$

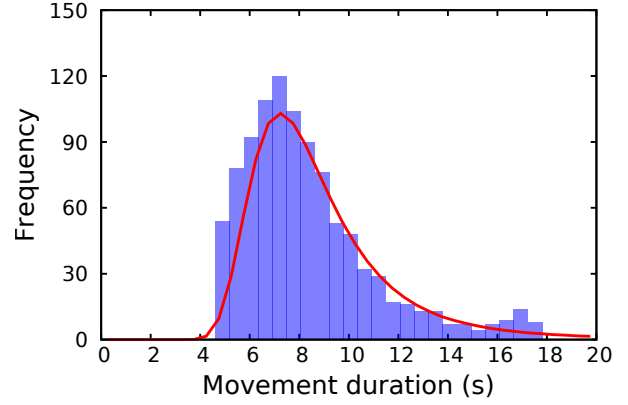


Figure 12: Frequency histogram of movement duration in a corner area estimated from numerical simulation (blue bars) and theoretically predicted by the ratio distribution (red solid line). We performed 1000 numerical simulations.

(25)

where $\mu_{s,c} = 7.65$ and $\sigma_{s,c} = 0.19$ are the mean and standard deviation of Gaussian distributed $s_c > 0$, and $\mu_{v,0} = 1.07$ and $\sigma_{v,0} = 0.29$ for Gaussian distributed $v_0 > 0$. The probability function of $t_{c,i}$ is given as

$$\begin{aligned} P(t_{c,i}) &= \int_{-\infty}^{+\infty} |v_0| f(s_c, v_0) dv_0 \\ &= \int_{-\infty}^{+\infty} |v_0| f(v_0 t_{c,i} \hat{v}_{avg}, v_0) dv_0 \\ &= \frac{1}{2\pi\sigma_{s,c}\sigma_{v,0}} \int_0^{+\infty} v_0 \times \\ &\exp \left\{ -\frac{1}{2} \left[\left(\frac{v_0 t_{c,i} \hat{v}_{avg} - \mu_{s,c}}{\sigma_{s,c}} \right)^2 + \left(\frac{v_0 - \mu_{v,0}}{\sigma_{v,0}} \right)^2 \right] \right\} dv_0. \end{aligned} \quad (26)$$

Based on Eq. (26), we theoretically predicted the frequency histogram of movement duration in a corner area and compared the result against one obtained from the numerical simulation, see Fig. 12. As can be seen from Fig. 12, the ratio distribution produced a right-skewed curve and the numerical simulation result is in good agreement with the theoretical prediction.

As shown in Eq. (21), the travel time in the straight corridor section j is given as

$$\begin{aligned} t_{s,j} &= \frac{\Delta s_j}{v_0} \left(\frac{2}{\hat{v}_{j-1} + \hat{v}_j} \right) \\ &= \frac{2\Delta s_j}{v_{j-1} + v_j}. \end{aligned} \quad (27)$$

Here, Δs_j is a fixed length of straight corridor section j , and the speed at the beginning and end points of the straight corridor section are denoted by v_{j-1} and v_j , respectively. It is

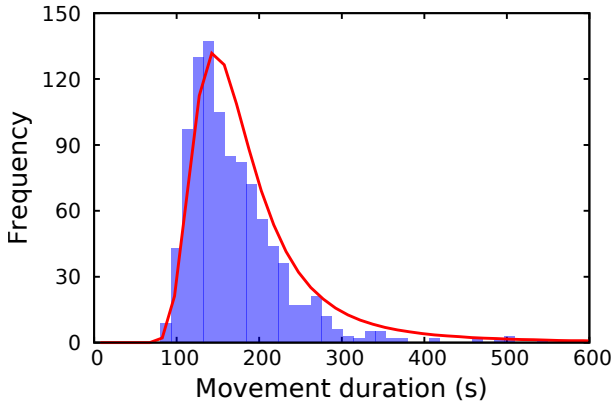


Figure 13: Frequency histogram of movement duration in the straight corridor sections (total length $s_j = 168$ m) estimated from numerical simulation (blue bars) and theoretically predicted by the ratio distribution (red solid line). We performed 1000 numerical simulations.

assumed that the value of v_{j-1} follows the normal distribution and the value of v_j is determined based on v_{j-1} and the fatigue effect. It can be inferred from Section 3.2 that the fatigue effect becomes considerable when the handler group travels several hundred meters. In a round trip, the total length of straight corridor sections is $s_j = \sum \Delta s_j = 168$ m, thus it may be reasonable to suppose that the difference between v_{j-1} and v_j is not significant. For simplicity, we approximate v_j to v_{j-1} and then simplify the equation of $t_{s,j}$ as a function of the total length of straight corridor sections s_j and the speed at the beginning point v_{j-1} :

$$t_{s,j} \approx \frac{s_j}{v_{j-1}}, \quad (28)$$

indicating that the distribution of $t_{s,j}$ is can be described by a reciprocal normal distribution. According to Gurarie *et al.* [34], the probability distribution function of $t_{s,j}$ is given as

$$P(t_{s,j}) = \frac{s_j}{\sqrt{2\pi}\sigma_{v,j-1}t_{s,j}} \exp \left[-\frac{1}{2} \left(\frac{s_j - \mu_{v,j-1}t_{s,j}}{\sigma_{v,j-1}t_{s,j}} \right)^2 \right], \quad (29)$$

where $\mu_{v,j-1} = 1.07$ and $\sigma_{v,j-1} = 0.29$ are mean and standard deviation of v_{j-1} , respectively. Based on Eq. (29), we theoretically predicted the frequency histogram of movement duration in the straight corridor and compared the result against one obtained from the numerical simulation, see Fig. 13. As can be seen from Fig. 13, the reciprocal normal distribution generated a right-skewed curve that is consistent with the numerical simulation result.

We computed an estimate of the movement duration for a round trip by summing the mode values of t_p , t_q , t_c , and t_s shown in Table 10, i.e., $T_{1,est} = 7.96 + 6.25 + 29.6 + 138.7 = 182.51$ s. One can notice that the total travel time in the corner and straight corridor areas (i.e., t_c and t_s) take a significant portion of movement duration $T_{1,est}$. Due to the right-skewed distributions of t_c and t_s , the spread of the simulated

Table 10
Mode values of parameters

parameters	mode	note
t_p	7.96	Normal distribution
t_q	6.25	Normal distribution
t_c	29.6	Ratio distribution
t_s	138.7	Reciprocal normal distribution

results presented in Figs. 9 and 11 is large. Given that the movement duration is inversely related to the entering speed, a small decrease in the entering speed might yield a large increase in the movement duration, extending the boundary of the histogram graph rightward.

References

- [1] T. Kretz, A. Grünebohm, M. Schreckenberg, Experimental study of pedestrian flow through a bottleneck, *Journal of Statistical Mechanics: Theory and Experiment* 2006 (2006) P10014+.
- [2] S. Hoogendoorn, W. Daamen, Pedestrian behavior at bottlenecks, *Transportation Science* 39 (2005) 147–159.
- [3] A. Seyfried, O. Passon, B. Steffen, M. Boltes, T. Rupprecht, W. Klingsch, New insights into pedestrian flow through bottlenecks, *Transportation Science* 43 (2009) 395–406.
- [4] F. Huo, W. Song, L. Chen, C. Liu, K. Liew, Experimental study on characteristics of pedestrian evacuation on stairs in a high-rise building, *Safety Science* 86 (2016) 165–173.
- [5] S. Burghardt, A. Seyfried, W. Klingsch, Performance of stairs—fundamental diagram and topographical measurements, *Transportation Research Part C: Emerging Technologies* 37 (2013) 268–278.
- [6] R. Nagai, M. Fukamachi, T. Nagatani, Evacuation of crawlers and walkers from corridor through an exit, *Physica A: Statistical Mechanics and its Applications* 367 (2006) 449–460.
- [7] R. Kady, J. Davis, The effect of occupant characteristics on crawling speed in evacuation, *Fire Safety Journal* 44 (2009) 451–457.
- [8] X. Lu, Z. Yang, G. Cimellaro, Z. Xu, Pedestrian evacuation simulation under the scenario with earthquake-induced falling debris, *Safety Science* 114 (2019) 61–71.
- [9] L. Rubadiri, D. Ndumu, J. Roberts, Predicting the evacuation capability of mobility-impaired occupants, *Fire Technology* 33 (1997) 32–53.
- [10] N. Strating, Evacuation of bedridden building occupants, Master's thesis, Eindhoven University of Technology, The Netherlands, 2013.
- [11] A. Hunt, E. Galea, P. Lawrence, An analysis and numerical simulation of the performance of trained hospital staff using movement assist devices to evacuate people with reduced mobility, *Fire and Materials* 39 (2015) 407–429.
- [12] L. Luo, Z. Fu, X. Zhou, K. Zhu, H. Yang, L. Yang, Fatigue effect on phase transition of pedestrian movement: experiment and simulation study, *Journal of Statistical Mechanics: Theory and Experiment* 2016 (2016) 103401.
- [13] X. Shi, Z. Ye, N. Shiwakoti, D. Tang, J. Lin, Examining effect of architectural adjustment on pedestrian crowd flow at bottleneck, *Physica A: Statistical Mechanics and its Applications* (2019) 350–364.
- [14] C. Dias, O. Ejtemai, M. Sarvi, N. Shiwakoti, Pedestrian walking characteristics through angled corridors: An experimental study, *Transportation Research Record* 2421 (2014) 41–50.
- [15] N. Shiwakoti, Y. Gong, X. Shi, Z. Ye, Examining influence of merging architectural features on pedestrian crowd movement, *Safety Science* 75 (2015) 15–22.
- [16] Aneurin Bevan Health Board, Guidance for the transfer of patients between wards and departments within hospitals, Technical Report, 2012.
- [17] Lund University Traffic Research Team, T-Analyst Software

- (<https://bitbucket.org/TrafficAndRoads/tanalyst/wiki/Manual>), 2019 (last accessed July 25, 2020).
- [18] A. Fyhri, H. Sundfør, T. Bjørnskau, A. Laureshyn, Safety in numbers for cyclists – conclusions from a multidisciplinary study of seasonal change in interplay and conflicts, *Accident Analysis & Prevention* 105 (2017) 124–133.
 - [19] S. Nielsen, R. Gade, T. Moeslund, H. Skov-Petersen, Taking the temperature of pedestrian movement in public spaces, in: W. Daamen, D. Duives, S. Hoogendoorn (Eds.), *The Conference on Pedestrian and Evacuation Dynamics 2014 (PED2014)*, Delft, The Netherlands, pp. 660–668.
 - [20] R. Tsai, A versatile camera calibration technique for high-accuracy 3D machine vision metrology using off-the-shelf TV cameras and lenses, *IEEE Journal on Robotics and Automation* 3 (1987) 323–344.
 - [21] J. Chen, J. Wang, J. Wang, X. Liu, T. Li, P. Lin, An experimental study of individual ascent speed on long stair, *Fire Technology* 53 (2017) 283–300.
 - [22] H. Hicheur, Q. C. Pham, G. Arechavaleta, J. P. Laumond, A. Berthoz, The formation of trajectories during goal-oriented locomotion in humans. I. A stereotyped behaviour, *European Journal of Neuroscience* 26 (2007) 2376–2390.
 - [23] C. Dias, R. Lovreglio, Calibrating cellular automaton models for pedestrians walking through corners, *Physics Letters A* 382 (2018) 1255–1261.
 - [24] N. Hogan, An organizing principle for a class of voluntary movements, *Journal of Neuroscience* 4 (1984) 2745–2754.
 - [25] Q. C. Pham, H. Hicheur, G. Arechavaleta, J. P. Laumond, A. Berthoz, The formation of trajectories during goal-oriented locomotion in humans. II. A maximum smoothness model, *European Journal of Neuroscience* 26 (2007) 2391–2403.
 - [26] C. Dias, M. Abdullah, M. Sarvi, R. Lovreglio, W. Alhajyaseen, Modeling and simulation of pedestrian movement planning around corners, *Sustainability* 11 (2019) 5501.
 - [27] R. Hocking, *Methods and applications of linear models: regression and the analysis of variance*, John Wiley & Sons, Hoboken, NJ, 3rd edition, 2013.
 - [28] E. Ronchi, E. D. Kuligowski, R. D. Peacock, P. A. Reneke, A probabilistic approach for the analysis of evacuation movement data, *Fire Safety Journal* 63 (2014) 69–78.
 - [29] G. Zhang, D. Huang, G. Zhu, G. Yuan, Probabilistic model for safe evacuation under the effect of uncertain factors in fire, *Safety Science* 93 (2017) 222–229.
 - [30] L. Y. Cooper, A concept for estimating available safe egress time in fires, *Fire Safety Journal* 5 (1983) 135–144.
 - [31] A. Hunt, E. Galea, P. Lawrence, I. Frost, S. Gwynne, Simulating movement devices used in hospital evacuation, *Fire Technology* (2020) 1–32.
 - [32] J. H. Curtiss, On the distribution of the quotient of two chance variables, *The Annals of Mathematical Statistics* 12 (1941) 409–421.
 - [33] M. D. Springer, *The algebra of random variables*, John Wiley & Sons, New York, NY, 1979.
 - [34] E. Gurarie, J. J. Anderson, R. W. Zabel, Continuous models of population-level heterogeneity inform analysis of animal dispersal and migration, *Ecology* 90 (2009) 2233–2242.